Refractive index properties of the retina accessed by multi-wavelength digital holographic microscopy

Álvaro Barroso*[a], Steffi Ketelhut[a], Peter Heiduschka[b], Gerburg Nettels-Hackert[b], Jürgen Schnekenburger[a], Björn Kemper[a]
[a]Biomedical Technology Center of the Medical Faculty, University of Muenster, Mendelstr. 17, D-48149, Germany;
[b]Dept. of Ophtalmology, University of Muenster Medical Centre, Domagkstr. 15, D-48149 Muenster, Germany

ABSTRACT

The refractive index (RI) of the retina and its dispersion are essential parameters in ophthalmologic imaging. However, the spatial RI distribution in retinal tissue is difficult to access. We explored the capabilities of multispectral quantitative phase imaging (QPI) with digital holographic microscopy (DHM) for label-free refractive index characterization of dissected murine retina. The retrieved tissue refractive indices are in agreement with previously reported values for living cells and dissected tissues. Moreover, the detected spatial refractive index distributions correlate with results from complementary conducted OCT investigations. In summary, multispectral DHM is a promising tool for label-free characterization of optical retina properties.

Keywords: digital holographic microscopy, quantitative phase imaging, multi-wavelength, hyperspectral imaging, retina, refractive index

1. INTRODUCTION

The refractive index (RI) of the retina and its dispersion are essential parameters in ophthalmologic imaging. On one hand, the RI determines the light propagation inside the tissue towards the photoreceptors. On the other hand, its spatial distribution reflects tissue structures by biophysical properties such as density of birefringence. Moreover, knowledge about wavelength dependency is crucial in high-resolution imaging, e.g. for dispersion compensation in optical coherence tomography (OCT). However, the spatial RI distribution in retinal tissue is difficult to access. Thus, in this work we explore the capabilities of quantitative phase imaging (QPI) for RI determination of murine retina utilizing digital holographic microscopy (DHM)[1]. DHM is an established tool that can be integrated as a module into common research microscopes[2]. In this way, DHM can be used for industrial non-destructive testing and label-free analysis of biological specimens like living cells or dissected tissues for multimodal label-free imaging[3]. For example, DHM has been utilized for quantification of migration[4] and motility[5] as well as for analysis of living cell cultures in three-dimensional environments[6,7], to mention few applications. Main restrictions of using laser light in DHM are coherence induced scattering, speckle, and parasitic reflections in the experimental setup. These disturbances affect the reconstructed amplitude and phase images and thus limit the measurement accuracy. Application of low coherent light, like for example light emitting diodes (LEDs), reduces such effects, but it requires special experimental arrangements or highly precise alignment of the optical equipment[8,9]. Following previous work[10–12], we have recently presented an approach that significantly decreases coherent noise in DHM by numerically superimposing monochromatic wave fields that were reconstructed from holograms acquired at different wavelengths of a tunable laser[13]. In this way, the robust alignment of a laser-based experimental setup can be combined with the noise reduction advantages of partial coherent light. In this study, we apply this approach for the analysis of the refractive index distribution of mouse retina sections.

*alvaro.barroso@uni-muenster.de

Three-Dimensional and Multidimensional Microscopy: Image Acquisition and Processing XXVI, edited by Thomas G. Brown, Tony Wilson, Proc. of SPIE Vol. 10883, 108830X · © 2019 SPIE · CCC code: 1605-7422/19/$18 · doi: 10.1117/12.2508976

2. MULTI-WAVELENGTH DIGITAL HOLOGRAPHIC MICROSCOPY

2.1 Sample preparation and experimental setup

The experiments were performed with a multi-wavelength modular DHM system implemented in a common inverted microscope (AE30, Motic, Hong Kong, China). Figure 1 shows a schematic of the employed experimental setup. The light source for QPI was a tunable supercontinuum laser (SuperK EXTREME EXR-9 combined with a Super Select nIR1/-acousto-optic tunable filter (AOTF) and a single mode fiber SuperK FD7 PM, NKT Photonics A/S, Birkerød, Denmark). The output light of the single mode fiber was converged into the optical path of the optical microscope using a beam splitter placed above the condenser lens (CL), which was adjusted to provide suitable Koehler illumination. A microscope objective lens (MO), a tube lens (TL), and a relay lens (RL) were used for magnification of the sample and for imaging it at the camera. A Michelson interferometer-based DHM configuration in which one of the mirrors was slightly tilted was used to generate digital off-axis holograms[14] that were recorded utilizing a standard industrial camera (DKM 23UP1300, The Imaging Source, Bremen, Germany). The Michelson interferometer configuration allows a robust and simplified alignment that is insensitive to changes of the object illumination and vibrations. Moreover, it can be operated with light with low coherences properties ($l_c \approx 50$ µm). For imaging of the sample, a 20x microscope lens (Zeiss LD Achroplan 20x/0.4 Korr) was used. Digital holograms were recorded at different wavelengths λ from 640 nm to 1100 nm.

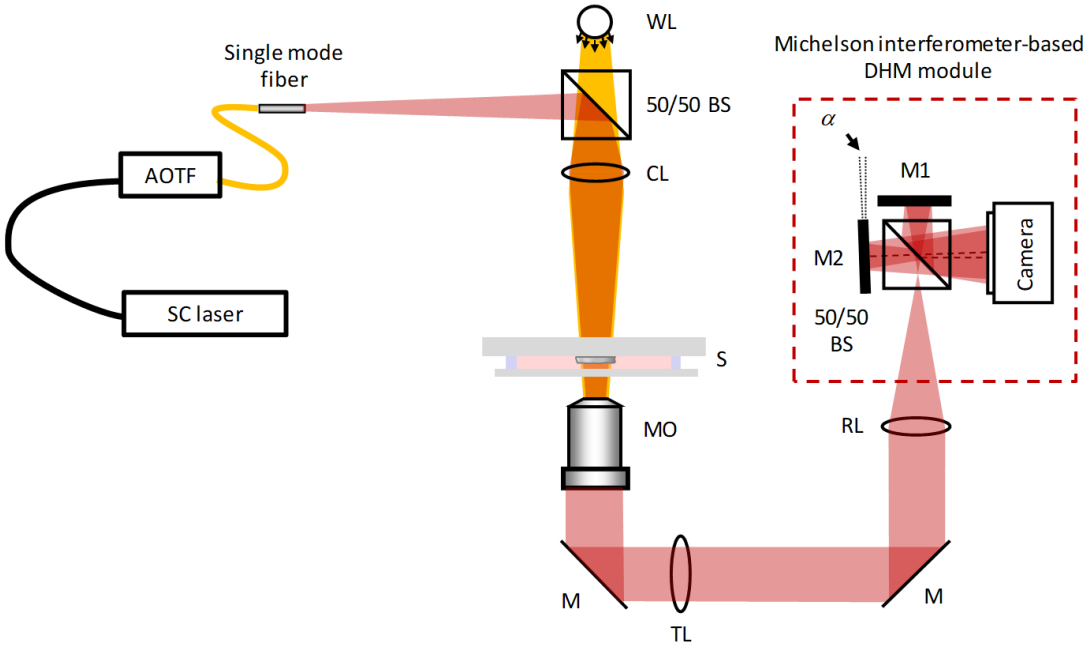

Figure 1. Concept for multi-spectral digital holographic microscopy. α: off-axis angle between object and reference wave, AOTF: Fiber coupled acousto-optic tunable filter, SC laser: fiber-coupled super continuum laser source; WL: white light illumination; BS: beam splitter; CL: condenser lens; S: sample; MO: microscope objective lens; M: mirror; TL: tube lens; RL: relay lens; CMOS: Complementary metal-oxide-semiconductor.

The sample preparation was carried out as follows. First, unstained cryostat mouse eye sections (5 µm thickness) were prepared on glass carriers and embedded in phosphate buffered saline (PBS). Other undesired parts of the eye, as the cornea, the sclera and choroid, were mechanically removed utilizing a scalpel. Next, the sample was washed several times in PBS to ensure that no dissected sample parts remained in the surrounding medium. Finally, for DHM measurements, the sample was covered with a cover slip.

2.2 Reconstruction of digital holograms for quantitative phase imaging of murine retina sections

The reconstruction of quantitative phase images from the acquired off-axis holograms was carried out by spatial phase shifting[15,16]. If the sample was not imaged sharply during hologram recording at different wavelength, numerical refocusing was applied[17]. Specially, numerical refocusing was necessary for near-infrared wavelengths, since the employed achromatic objective was designed to correct for chromatic aberration in wavelengths of the visible range. Figure 2 illustrates the performance of multi-wavelength DHM for quantitative phase imaging of dissected mouse retina. In particular, to minimize possible unwrapping errors resulting from the thickness of the sample tissue, several digital holograms were acquired at different wavelengths in the interval 800-850 nm in steps of $\Delta\lambda$=10 nm. This wavelength range is especially important in high resolution ophthalmological imaging with optical coherence tomography (OCT).

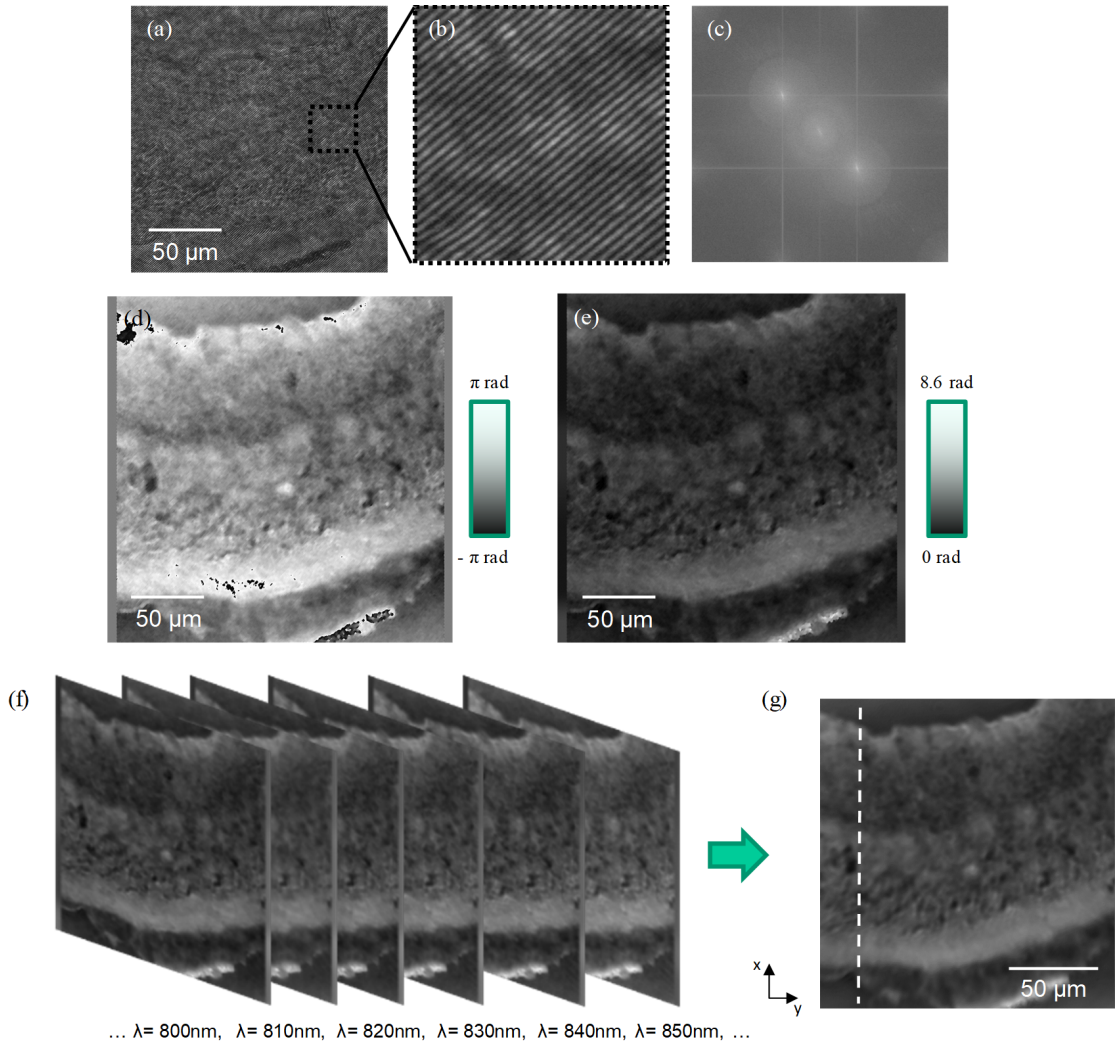

Figure 2. Example for evaluation of reconstruction of multi-wavelength digital holograms and corresponding quantitative phase images (QPI): (a): digital off-axis hologram of a region of a mouse retina section. (b): Enlarged spatial carrier fringe pattern of (a). (c) Two dimensional frequency spectrum of (a). (d): Quantitative phase contrast image (mod 2π). (e): Unwrapped phase distribution. (f): Stack of QPI of the same region that were obtained from digital holograms at different wavelengths. (g) Averaged QPI obtained by numerically superimposing the stack of QPIs in (f). The dashed line indicates the cross section evaluated in Figure 3 for refractive index determination.

3. REFRACTIVE INDEX DETERMINATION OF MURINE RETINA SECTIONS

As it can be observed in Fig.2, the different cell layers that form the retina modulate the phase distribution of the retina. In order from the eye lens to the choroid, these layers are: the ganglion cell layer (GCL), the inner plexiform layer (IPL), the inner nuclear layer (INL), the outer plexiform layer (OPL), the outer nuclear layer (ONL), the inner and outer segments (IS and OS, respectively), and the retinal pigment epithelium (RPE)[18]. In order to investigate the refractive index of each layer, one can recall the relation between the measured quantitative phase delay $\Delta\varphi_S$ of the object, the thickness and the refractive index of the sample:

$$\Delta\varphi_S = \frac{2\pi}{\lambda}\left(n_S - n_{\text{medium}}\right)d_S, \tag{1}$$

where λ is the applied laser wavelength, d_S represents the thickness of the sample, n_s the integral refractive index of the sample, and n_{medium} the refractive index of the surrounding medium.

With information about the thickness of the sample tissue, and regarding the optical dispersion of the surrounding medium, the information of the reconstructed object wave phase can be applied for determination of the integral refractive index of the specimen:

$$n_S = n_{\text{medium}} + \frac{\lambda}{2\pi d_S}\Delta\varphi_S. \tag{2}$$

Figure 3 shows the measured refractive index of the retina $n_s = n_{\text{retina}}$ along the cross section indicated with the dashed line in Fig. 2(g). The detected spatial refractive index distributions correlate with reported OCT and histology images of mouse retina.[19] Due to the high refractive index different between consecutive cell layers, the refractive index of the GCL, the INL, the ONL and the RPE can be clearly detected. The refractive indices that are obtained for these cell layers are in well agreement with previously reported values for living cells and dissected tissues[20,21].

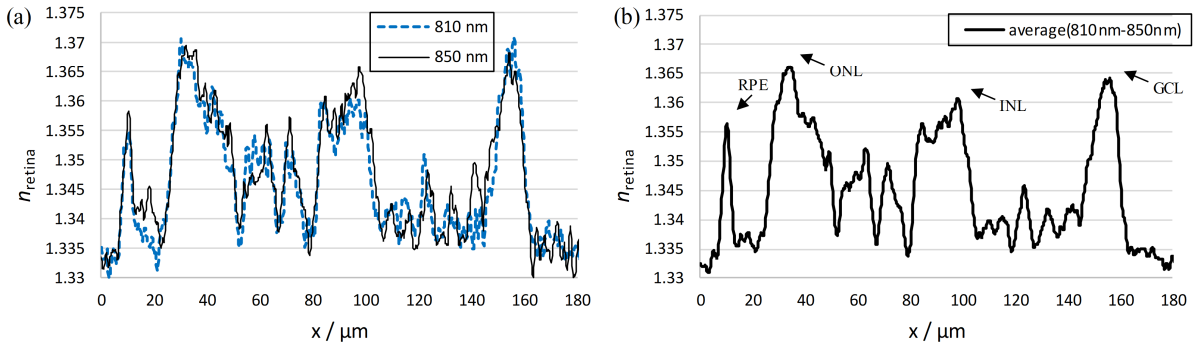

Figure 3. (a) Calculated integral refractive index n_{retina} of the retina through the cross section indicated with a dashed line in Fig. 2(g) for the specific wavelengths λ = 810 nm and λ = 850 nm, and (b) the averaged value of the refractive index using QPIs from λ = 810 nm to λ = 850 nm in steps of $\Delta\lambda$ = 10 nm.

4. CONCLUSIONS

In summary, we have reported a novel method for label-free refractive index characterization of dissected murine retina based on multispectral quantitative phase imaging (QPI) using digital holographic microscopy (DHM). By acquiring digital off-axis holograms with a tunable laser, our approach enables to investigate the refractive index distribution of retina at different wavelengths. Results from an unstained cryostat mouse retina section demonstrate that the method allows detection and quantitative analysis of the refractive index of the different tissue layers that form the retina. In conclusion, quantitative phase imaging using multi-spectral DHM is a promising tool for label-free characterization of optical retina properties.

ACKNOWLEDGEMENTS

Funding by the European Union (Horizon 2020 Project GALAHAD, no: 732613) is gratefully acknowledged.

REFERENCES

[1] Cuche, E., Marquet, P. and Depeursinge, C., "Simultaneous amplitude-contrast and quantitative phase-contrast microscopy by numerical reconstruction of Fresnel off-axis holograms," Appl. Opt. **38**(34), 6994–7001 (1999).

[2] Kemper, B., Carl, D., Höink, A., von Bally, G., Bredebusch, I. and Schnekenburger, J., "Modular digital holographic microscopy system for marker free quantitative phase contrast imaging of living cells," 61910T (2006).

[3] Bettenworth, D., Lenz, P., Krausewitz, P., Brückner, M., Ketelhut, S., Domagk, D. and Kemper, B., "Quantitative stain-free and continuous multimodal monitoring of wound healing in vitro with digital holographic microscopy," PLoS One **9**(9) (2014).

[4] Kemper, B., Bauwens, A., Vollmer, A., Ketelhut, S., Langehanenberg, P., Müthing, J., Karch, H. and von Bally, G., "Label-free quantitative cell division monitoring of endothelial cells by digital holographic microscopy," J. Biomed. Opt. **15**(3), 036009 (2010).

[5] Sridharan, S., Mir, M. and Popescu, G., "Simultaneous optical measurements of cell motility and growth," Biomed. Opt. Express **2**(10), 2815 (2011).

[6] Langehanenberg, P., Ivanova, L., Bernhardt, I., Ketelhut, S., Vollmer, A., Dirksen, D., Georgiev, G., von Bally, G. and Kemper, B., "Automated three-dimensional tracking of living cells by digital holographic microscopy.," J. Biomed. Opt. **14**(1), 014018 (2009).

[7] Kus, A., Dudek, M., Kemper, B., Kujawinska, M. and Vollmer, A., "Tomographic phase microscopy of living three-dimensional cell cultures," J. Biomed. Opt. **19**(4), 046009 (2014).

[8] Kemper, B., Stürwald, S., Remmersmann, C., Langehanenberg, P. and von Bally, G., "Characterisation of light emitting diodes (LEDs) for application in digital holographic microscopy for inspection of micro and nanostructured surfaces," Opt. Lasers Eng. **46**(7), 499–507 (2008).

[9] Langehanenberg, P., Bally, G. Von and Kemper, B., "Application of partially coherent light in live cell imaging with digital holographic microscopy," J. Mod. Opt. **57**(9), 709–717 (2010).

[10] Nomura, T., Okamura, M., Nitanai, E. and Numata, T., "Image quality improvement of digital holography by superposition of reconstructed images obtained by multiple wavelengths," Appl. Opt. **47**(19), D38--D43 (2008).

[11] Kosmeier, S., Langehanenberg, P., Przibilla, S., von Bally, G. and Kemper, B., "Multi-Wavelength Digital Holographic Microscopy for High Resolution Inspection of Surfaces and Imaging of Phase Specimen," Opt. Micro- Nanometrology Iii **7718**, 1–7 (2010).

[12] Kosmeier, S., Langehanenberg, P., Von Bally, G. and Kemper, B., "Reduction of parasitic interferences in digital holographic microscopy by numerically decreased coherence length," Appl. Phys. B Lasers Opt. **106**(1), 107–115 (2012).

[13] Barroso, Á., Ketelhut, S., Heiduschka, P., Kastl, L., Schnekenburger, J. and Kemper, B., "Hyperspectral digital holographic microscopy approach for reduction of coherence induced disturbances in quantitative phase imaging of biological specimens," Proc. SPIE **10834**(Speckle 2018: VII International Conference on Speckle Metrology), 108340I (2018).

[14] Kemper, B., Vollmer, A., Rommel, C. E., Schnekenburger, J. and von Bally, G., "Simplified approach for quantitative digital holographic phase contrast imaging of living cells.," J. Biomed. Opt. **16**(February), 026014 (2011).

[15] Carl, D., Kemper, B., Wernicke, G. and von Bally, G., "Parameter-optimized digital holographic microscope for high-resolution living-cell analysis.," Appl. Opt. **43**(36), 6536–6544 (2004).

[16] Kemper, B., Carl, D., Schnekenburger, J., Bredebusch, I., Schäfer, M., Domschke, W. and von Bally, G., "Investigation of living pancreas tumor cells by digital holographic microscopy," J. Biomed. Opt. **11**(3), 034005 (2006).

[17] Langehanenberg, P., Kemper, B., Dirksen, D. and von Bally, G., "Autofocusing in digital holographic phase contrast microscopy on pure phase objects for live cell imaging," Appl. Opt. **47**(19), D176 (2008).

[18] Veleri, S., Lazar, C. H., Chang, B., Sieving, P. A., Banin, E. and Swaroop, A., "Biology and therapy of inherited retinal degenerative disease: insights from mouse models," Dis. Model. Mech. **8**(2), 109–129 (2015).

[19] Kastl, L., Isbach, M., Dirksen, D., Schnekenburger, J. and Kemper, B., "Quantitative phase imaging for cell culture quality control," Cytom. Part A **91**(5), 470–481 (2017).

[20] Harper, D. J., Augustin, M., Lichtenegger, A., Eugui, P., Reyes, C., Glösmann, M., Hitzenberger, C. K. and Baumann, B., "White light polarization sensitive optical coherence tomography for sub-micron axial resolution and spectroscopic contrast in the murine retina," Biomed. Opt. Express **9**(5), 2115 (2018).

[21] Lenz, P., Bettenworth, D., Krausewitz, P., Brückner, M., Ketelhut, S., Von Bally, G., Domagk, D. and Kemper, B., "Digital holographic microscopy quantifies the degree of inflammation in experimental colitis," Integr. Biol. **5**(3), 624–630 (2013).